Acta Chemica Scandinavica, 1996: 50: 1–5
Printed in Belgium – all rights reserved

ACTA
CHEMICA SCANDINAVICA
ISSN 0904–213X

Synthesis, Crystal Structure and Photochemical Study of Bis(2,4,6-triphenylpyryllium)hexamolybdate (TPPM) and $[n\text{-Bu}_4N]_2[Mo_6O_{19}]$ · (TBAM)

Xue-Xiang Xu,[†,a] Xiao-Zeng You*[,a] and Xin Wang*[,b]

[a]Coordination Chemistry Institute, Sate Key Laboratory of Coordination Chemistry, Nanjing University, Centre for Advanced Studies in Science and Technology of Microstructures, Nanjing 210093, People's Republic of China and [b]Centre of Analysis Research, Lanzhou University, Lanzhou 730000, People's Republic of China

Xu, X.-X., You, X.-Z., Wang, X., 1996. Synthesis, Crystal Structure and Photochemical Study of Bis(2,4,6-triphenylpyryllium)hexamolybdate (TPPM) and $[n\text{-Bu}_4N]_2[Mo_6O_{19}]$·(TBAM). – Acta Chem. Scand. 50: 1–5 © Acta Chemica Scandinavica 1996.

A complex between an organic photosensitizer, **TPP**, and the isopolyanion $Mo_6O_{19}^{2-}$, of stoicheiometry $(TPP)_2Mo_6O_{19}$ (**TPPM**), has been characterized in solution. The irradiation of the low-energy absorption bands of **TPPM** in solution results in immediate photochromism, a process which is reversible and repeatable. $Mo_6O_{19}^{2-}$ can quench the fluorescence of **TPP**. Comparison of the photochromism of both **TPPM** and $[n\text{-Bu}_4N]_2[Mo_6O_{19}]$ (**TBAM**) show that **TPPM** has more intense photochromism and a faster fade rate than that of **TBAM**. The photochromism process of **TBAM** is irreversible. In the crystal stack **TPP** cations form a stack, and the Mo_6O_{19} anions form parallel columns alternately.

Recent work has highlighted the ability for photochromism of well known polyoxoanions conjugated with organic molecules.[1–7] However, photochromism involving these compounds is not truly reversible. In order to prepare reversible photochromic materials, we have chosen photosensitive organic molecules as donor and Type I polyoxometalate anions having easily reduced properties[8] as acceptor. Such anions are still of interest because of their high electron acceptor capability.[9] We report here a new reversible photochromic charge-transfer salt using photosensitive triphenylpyryllium (**TPP**) as donor and the hexamolybdate dianion ($Mo_6O_{19}^{2-}$), having the Lindquist structure, as acceptor.[10] Although the photochemistry of $[n\text{-Bu}_4N]_2[Mo_6O_{19}]$ (**TBAM**) under flash photolysis has been published previously,[11] no photochromism has been reported under ultraviolet irradiation. In this paper the photochromism of **TBAM** in DMF solution is examined and compared with that of **TPPM**.

Experimental

All materials were of reagent grade and used without further purification. $[n\text{-Bu}_4N]_2[Mo_6O_{19}]$[12] and $TPPClO_4$[13] were prepared and purified according to literature procedures.

Elemental analyses were performed on a Perkin-Elmer 240C instrument. Electronic spectra were recorded on a Shimadzu UV-3100. The ESR spectra were obtained on a Bruker ER 200D spectrometer. The emission spectra were obtained using a RF-450 spectrofluorometer (Shanghai, China).

*Synthesis of $[TPP]_2[Mo_6O_{19}]$ (***TPPM***).* The title compound has been obtained as a yellow precipitate by reacting a stoicheiometric amount of $[n\text{-Bu}_4N]_2[Mo_6O_{19}]$ with $(TPP)ClO_4$ in acetonitrile solution. Single crystals were obtained by a diffusion method. Anal: Calcd. for $C_{46}H_{34}Mo_6O_{21}$: C, 36.87; H, 2.29. Found: C, 36.65; H, 2.13.

Determination of the crystal structure. A single crystal with the approximate dimensions $0.40 \times 0.25 \times 0.30$ mm was mounted on a glass fibre. All the intensity data were collected on an Enraf-Nonius CAD4 diffractometer using graphite-monochromated Cu Kα radiation ($\lambda = 1.5418$ Å) with a scan mode of ω–2Θ. Independent reflections (3578) were collected in the range $2 < 2\Theta < 116°$, and 2598 reflections with $I > 3\sigma(I)$ were used for further computation. All data were corrected for Lorentz and polarization effects, and empirical absorption corrections, based on ψ scans, were applied.

[†] Present address: Institute of Chemistry, Academia Sinica, Beijing 100080, People's Republic of China.
* To whom correspondence should be addressed.

TPPM is monoclinic, space group $C2/c$, $M_r = 1498.5$, with the cell dimensions $a = 19.769(2)$, $b = 14.352(3)$, $c = 16.868(2)$ Å, $\beta = 99.99(3)°$, $V = 4713.4$ Å^3, $Z = 4$, $D_{calc} = 2.111$ g cm^{-3}, $F(000) = 2920$, $\mu = 136.8$ cm^{-1}. The structure analysis was performed on a PDP 11/44 computer with an SDP program.[14] The positions of all the molybdenum atoms were determined by direct methods. The positions of other non-hydrogen atoms were revealed by difference Fourier syntheses. The hydrogen atoms, located in a difference map and fixed with isotropic $B = 5.0$ Å^2, were included as a fixed contribution. The structure was refined with unit weights by full-matrix least-squares methods with anisotropic thermal factors for all non-hydrogen atoms. Refinement converged to a final $R = 0.078$ and $R_w = 0.079$ for the 2598 observed reflections.

Results and discussion

Synthesis of **TPPM**. When an acetonitrile solution of the $TPPClO_4$ and isopolyoxomolybdate $Mo_6O_{19}^{2-}$ are mixed, a new material far less soluble in acetonitrile than either of the components precipitates from the solution. This complex between the isopolymolybdate and the organic substrate, $TPP_2[Mo_6O_{19}]$ (**TPPM**), can be recrystallized from DMF.

Photochemistry of **TBAM** *and* **TPPM** *in solution*. Figure 1 shows the absorption spectra of a DMF solution of **TBAM** before dianion formation, after 60 min of irradiation of the above solution, and after the solution had faded. On irradiation, the DMF solution of **TBAM** shows broad absorption bands at 660 and 820 nm in electronic spectra, which indicate that $Mo^{V}Mo_5^{VI}O_{19}^{3-}$ were formed. The absorption spectrum of Mo^{V} obtained in this work is very different in shape and peak position from that of produced by electrolysis of $Mo_6O_{19}^{2-}$ in DMF.[12] The band at 820 nm is assigned to the $^2B_2 \rightarrow {}^2E$ IVCT transitions (band B).[10,12] In the electrolysis spectrum Mo^{V} shows an IVCT transition of shoulder band A at 1110 nm,[12] but has no band in the photochemical reduced Mo^{V}. This indicates that band A may have merged with band B.[10] This case also occurred in other polyoxometalates on photochemical reduction.[1,4] The band at 660 nm may also be ascribed to band B, which did not occur in the spectrum of electroreduced Mo^{V},[12] but was observed in the spectrum of photoreduced $[Mo_7O_{24}]^{6-}$.[1] The colored solution shows a two-stage transient decay of the photochromer, and its first-order fade rate constants k_1 and k_2 are 1.8×10^{-4} and 3.1×10^{-5} s^{-1}, respectively, by spectroscopic methods. The colored solution gave rise to a single intense ESR signal at 293 K ($g = 1.923$, $\Delta H = 52$ G) due to Mo^{V}.[12] **TBAM** was not equivalent to that obtained prior to photolysis; the maximum absorption shifted from 327 to 295 nm owing to photochemically induced changes. This implies that certain Mo^{V} species or a protonated polyoxometalate[6] may exist in the faded solution. The primary photochemical reactions can be expressed as follows:[11]

$$Mo_6O_{19}^{2-} \overset{h\nu}{\rightleftharpoons} (Mo_6O_{19}^{2-})^* \quad (1)$$

$$(Mo_6O_{19}^{2-})^* + SH_2 \rightleftharpoons Mo_6O_{19}^{3-} + \cdot SH + H^+ \quad (2)$$

or

$$(Mo_6O_{19}^{2-})^* + SH_2 \rightleftharpoons HMo^{V}Mo_5O_{19}^{2-} + \cdot SH \quad (3)$$

where SH_2 and $\cdot SH$ represent DMF and $HCON(CH_3)CH_2\cdot$, respectively. The $\cdot SH$ radical may disappear by radical recombinant or self-decomposition.[15] Because of the low quantum yield of Mo^{V},[11] photochromism of **TBAM** has not been observed in CH_3CN solution under ultraviolet light irradiation.

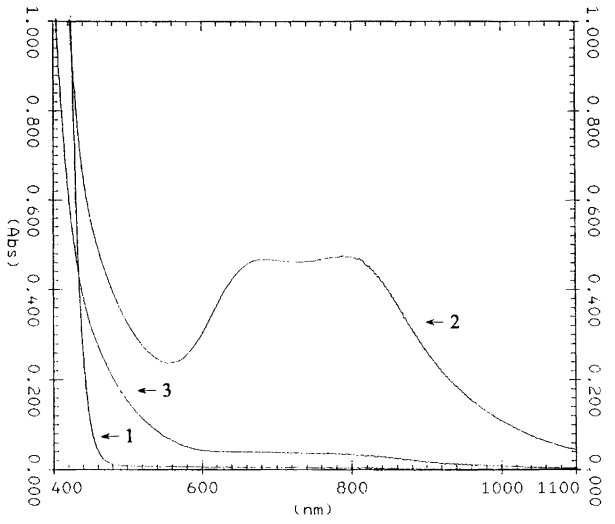

Fig. 1. Absorption spectra of $[n\text{-}Bu_4N]_2[Mo_6O_{19}]$ (in DMF, $5_4 \times 10^{-3}$ M) in a 10 mm cell at room temperature, irradiation with a 500 W Xe lamp using cut-off filters ≥ 300 nm for 60 min, (1) before irradiation, (2) after irradiation, and (3) after fade.

Figure 2 shows the electronic absorption spectra of **TPP** and **TPPM** before and after irradiation. On irradiation, although **TPP** exhibits photochromism with a maximum absorption band at 483 nm, the **TPPM** displays more intense photochromism. The absorption spectrum of irradiated **TPPM** is very similar to that of **TBAM**, but its photochromism is more intense than that of the latter. The of photochromism of **TPPM** is reversible and can be repeated many times, but it fades away faster than **TBAM**; the rate constants are $k_1 = 3.8 \times 10^{-3}$ and $k_2 = 5.2 \times 10^{-5}$, respectively. In the resulting colored solution no ESR signal could be observed.

Figure 3 shows the fluorescence spectra of **TPP** and **TPPM**. The **TPP** exhibits intense fluorescence ($\lambda_{max} = 475$ nm),[16] but the fluorescence intensity of **TPPM** is only 45% that of **TPP**. This indicates that the

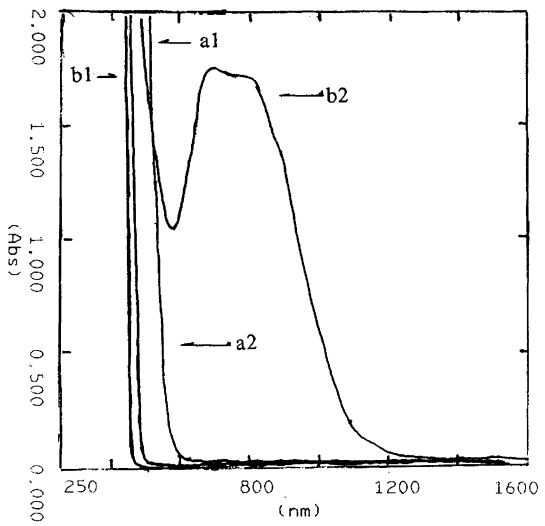

Fig. 2. Solution electronic spectra of the $(TPP)ClO_4$ (a) and the title complex TPPM (b). Both 5×10^{-3} M (DMF). The condition of irradiation is the same as that of $[n\text{-}Bu_4N]_2[Mo_6O_{19}]$, (1) before and (2) after irradiation.

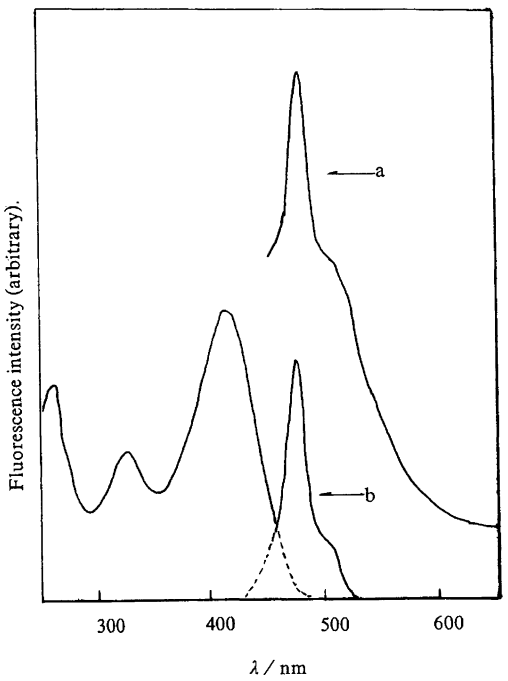

Fig. 3. Emission spectra of $(TPP)ClO_4$ (a) (2×10^{-5}) and TPPM (b) $(1\times10^{-5}$ M) (in DMF solution, $\lambda_{ex}=417$ nm) at room temperature. The excitation spectrum of TPPM is given on the left-hand side.

fluorescence of **TPP** can be quenched by $Mo_6O_{19}^{2-}$. The photochromism process and the quenching mechanism of **TPPM** may be summarized as follows:[17]

fluorescence:

$$TPP^+ \overset{h\nu}{\rightleftharpoons} (TPP^+)^* \qquad (4)$$

quenching:

$$(TPP^+)^* + Mo_6O_{19}^{2-} \rightarrow TPP^{+\cdot} + (Mo_6O_{19}^{2-})^* \qquad (5)$$

photochromism:

$$(TPP^+)^* + SH_2 \rightarrow TPP^{\cdot} + SH_2^{+\cdot} \qquad (6)$$

The $(Mo_6O_{19}^{2-})^*$ state in **TPPM** can be obtained by energy transfer with ultraviolet irradiation from excited $(\mathbf{TPP}^+)^*$, which results in quenching of the fluorescence of $(\mathbf{TPP}^+)^*$. From the redox potentials of $\mathbf{TPP}^+$ $(-0.37$ V)[18] and $Mo_6O_{19}^{2-}$ $(-0.83$ V),[19] it can be expected that $\mathbf{TPP}^+$ may interact with $Mo_6O_{19}^{3-}$:

$$Mo_6O_{19}^{3-} + TPP^+ \rightarrow Mo_6O_{19}^{2-} + TPP^{\cdot} \qquad (7)$$

Because the photochromism of **TPP** is reversible,[17] the all photochromic procedures of **TPPM** are also reversible.

From the results outlined above, it can be expected that the quantum yield for the formation of the reduced hexamolybdate will increase by energy transfer from excited **TPP**. The fact that **TPPM** shows reversible photochromism and a faster fade rate may be due to interactions between the $\mathbf{TPP}^+$ radical and $Mo_6O_{19}^{3-}$.

Structural studies. The atomic coordinates of non-hydrogen atoms, bond distances and angles are listed in Tables 1, 2 and 3, respectively. The molecular structure and crystal structure of the title complex are displayed in Figs. 4 and 5.

The average Mo–O bond distances in $[Mo_6O_{19}]^{2-}$ are similar to those reported previously,[20,21] i.e. 1.680(6) Å for $Mo\text{–}O_t$ (terminal), 1.917(4) Å for $Mo\text{–}O_b$ (bridging) and 2.312(1) Å for $Mo\text{–}O_c$ (central).

The pyryllium ring is almost planar, with a maximum deviation of 0.018 Å from the best plane. The bond angle of oxygen is 124.1(7)° and the two C–O bonds are

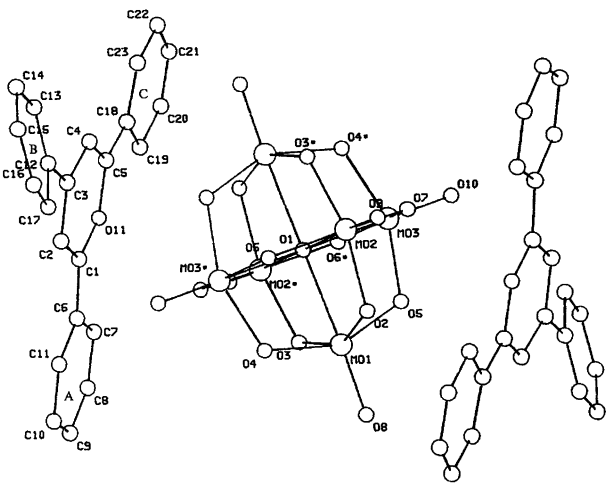

Fig. 4. Molecular structure of $[TPP]_2[Mo_6O_{19}]$.

Table 1. The non-hydrogen atomic coordinates of $[TPP]_2Mo_6O_{19}$.

Atom	*x*	*y*	*z*	*B*/Å
Mo1	0.23473(8)	0.1149(1)	0.5701(1)	2.07(3)
Mo2	0.13609(7)	0.2879(1)	0.4961(1)	1.99(3)[a]
Mo3	0.27897(8)	0.3296(1)	0.6203(1)	2.17(3)
O1	0.250	0.250	0.500	1.6(3)
O2	0.1459(5)	0.1698(9)	0.5523(8)	1.7(3)[a]
O3	0.3296(5)	0.1110(9)	0.5594(9)	2.2(3)
O4	0.2146(7)	0.0779(9)	0.4582(9)	2.6(3)
O5	0.2615(6)	0.205(1)	0.652(8)	2.5(3)
O6	0.1341(5)	0.217(1)	0.3980(8)	2.3(3)[a]
O7	0.1826(5)	0.344(1)	0.5962(8)	2.5(3)[a]
O8	0.2243(7)	0.015(1)	0.618(1)	3.8(4)
O9	0.0528(4)	0.311(1)	0.4944(9)	3.2(3)
O10	0.29990(7)	0.388(1)	0.7082(9)	3.8(4)
O11	0.4173(7)	0.239(1)	0.2943(9)	3.1(3)
C1	0.382(1)	0.166(2)	0.260(1)	2.6(4)
C2	0.324(1)	0.184(2)	0.2202(1)	2.8(5)
C3	0.303(1)	0.274(2)	0.184(1)	2.8(5)
C4	0.342(1)	0.348(2)	0.223(4)	2.5(4)
C5	0.398(1)	0.329(2)	0.279(1)	2.8(5)
C6	0.4067(8)	0.076(2)	0.286(1)	2.3(4)[a]
C7	0.467(8)	0.065(2)	0.343(2)	4.2(6)[a]
C8	0.492(1)	−0.021(2)	0.362(2)	5.3(7)[a]
C9	0.459(1)	−0.100(2)	0.334(2)	5.3(7)
C10	0.400(2)	−0.091(2)	0.279(2)	5.7(7)
C11	0.372(1)	−0.004(2)	0.2557(2)	4.7(6)
C12	0.264(1)	0.296(2)	0.112(1)	2.9(5)
C13	0.233(1)	0.374(2)	0.083(2)	5.1(7)
C14	0.172(1)	0.394(2)	0.023(2)	5.8(7)
C15	0.123(1)	0.326(2)	0.013(2)	5.2(7)
C16	0.129(1)	0.246(2)	0.052(2)	5.3(7)
C17	0.188(1)	0.222(2)	0.107(2)	4.0(6)
C18	0.4439(9)	0.399(2)	0.320(1)	2.3(4)
C19	0.501(1)	0.369(2)	0.373(2)	4.8(62)
C20	0.545(1)	0.443(2)	0.412(2)	6.1(8)
C21	0.531(1)	0.529(2)	0.401(2)	5.0(6)
C22	0.475(2)	0.560(2)	0.350(2)	5.7(8)
C23	0.420(1)	0.493(2)	0.311(2)	4.0(6)

[a]Isotropic thermal factors.

Table 3. Bond angles of $[TTP]_2Mo_6O_{19}$ (in °).

O1–Mo1–O2	76.8(2)	O5–Mo3–O10	104.1(3)
O1–Mo1–O3	71.1(2)	O6–Mo3–O7	154.3(2)
O1–Mo1–O4	75.8(1)	O6–Mo3–O10	103.6(2)
O1–Mo1–O5	76.1(1)	O7–Mo3–O10	102.1(2)
O1–Mo1–O8	178.2(2)	C1–O11–C5	124.1(7)
O2–Mo1–O3	152.9(3)	O11–C1–C2	117.8(5)
O2–Mo1–O4	86.1(2)	O11–C1–C6	117.1(7)
O2–Mo1–O5	88.1(2)	C2–C1–C6	125.0(6)
O2–Mo1–O8	104.1(3)	C1–C2–C3	120.2(6)
O3–Mo1–O4	86.5(2)	C2–C3–C4	118.7(7)
O3–Mo1–O5	86.3(2)	C2–C3–C12	120.2(6)
O3–Mo1–O8	103.0(2)	C4–C3–C12	121.1(6)
O4–Mo1–O5	151.9(2)	C3–C4–C5	120.0(6)
O4–Mo1–O8	102.5(3)	O11–C5–C4	119.2(8)
O5–Mo1–O8	105.6(3)	O11–C5–C18	116(1)
O1–Mo2–O2	76.5(3)	C4–C5–C8	124.3(7)
O1–Mo2–O3	76.5(3)	C1–C6–C7	120.8(7)
O1–Mo2–O6	77.04(9)	C1–C6–C11	121.7(8)
O1–Mo2–O7	76.1(2)	C7–C6–C11	117.7(6)
O1–Mo2–O9	177.8(1)	C6–C7–C	119.4(7)
O2–Mo2–O3	152.9(4)	C7–C8–C9	123.4(8)
O2–Mo2–O6	86.8(2)	C8–C9–C10	118.2(7)
O2–Mo2–O7	86.7(2)	C9–C10–C11	120.6(7)
O2–Mo2–O9	101.4(2)	C6–C11–C10	120.3(7)
O3–Mo2–O6	86.3(2)	C3–C12–C13	121.7(8)
O3–Mo2–O7	87.7(2)	C3–C12–C17	118.3(7)
O3–Mo2–O9	105.8(3)	C13–C12–C17	119.9(8)
O6–Mo2–O7	153.2(2)	C12–C13–C14	123(2)
O6–Mo2–O9	102.5(2)	C13–C14–C15	115(2)
O7–Mo2–O9	104.3(2)	C14–C15–C16	123(2)
O1–Mo3–O4	76.6(1)	C15–C16–C17	123.1(9)
O1–Mo3–O5	75.8(1)	C12–C17–C16	115.3(7)
O1–Mo3–O6	77.3(1)	C5–C18–C19	117.5(9)
O1–Mo3–O7	77.2(1)	C5–C18–C23	122.0(9)
O1–Mo3–O10	179.2(2)	C19–C18–C23	120(1)
O4–Mo3–O5	152.5(2)	C18–C29–C20	114.9(9)
O4–Mo3–O6	87.8(2)	C19–C20–C21	122.5(9)
O4–Mo3–O7	87.8(2)	C20–C21–C22	124(1)
O4–Mo3–O10	103.5(2)	C21–C22–C23	116.6(8)
O5–Mo3–O6	85.9(1)	C18–C23–C22	121.6(8)
O5–Mo3–O7	86.3(2)		

1.338(8) and 1.356(8) Å, respectively, which differ from that of the **TPP**–tetracyanopropenide (**TPP–TCP**)[22] [122.5(3)° and 1.355(4) Å]. The C–C bond lengths of pyryllium ring are in the accepted range for a benzene ring, which is different from the of **TPP–TCP**, where the C–C bond lengths are significantly different from that of a benzene ring. This indicates that the electron delocalization of the pyryllium ring in **TPPM** is greater than that of **TPP–TCP**. The electron delocalization may also be

Table 2. Bond distances of $[TTP]_2Mo_6O_{19}$ (in Å).

Mo1–O1	2.3178(7)	Mo3–O6	1.918(4)	C8–C9	1.34(2)
Mo1–O2	1.901(7)	Mo3–O7	1.889(7)	C9–C10	1.36(2)
Mo1–O3	1.92(1)	Mo3–O10	1.668(7)	C10–C11	1.39(1)
Mo1–O4	1.935(3)	O11–C1	1.338(8)	C12–C13	1.33(1)
Mo1–O5	1.897(3)	O11–C5	1.356(9)	C12–C17	1.46(1)
Mo1–O8	1.676(4)	C1–C2	1.40(1)	C13–C14	1.44(1)
Mo2–O1	2.3064(6)	C1–C6	1.432(9)	C14–C15	1.38(2)
Mo2–O2	1.935(5)	C2–C3	1.388(7)	C15–C16	1.32(2)
Mo2–O3	1.913(6)	C3–C4	1.410(9)	C16–C17	1.40(1)
Mo2–O6	1.936(4)	C3–C12	1.48(1)	C18–C19	1.39(2)
Mo2–O7	1.950(4)	C4–C5	1.36(1)	C18–C23	1.37(1)
Mo2–O9	1.676(6)	C5–C18	1.44(1)	C19–C20	1.46(2)
Mo3–O1	2.3127(5)	C6–C7	1.40(1)	C20–C21	1.27(1)
Mo3–O4	1.895(4)	C6–C11	1.38(2)	C21–C22	1.36(1)
Mo3–O5	1.920(4)	C7–C8	1.36(2)	C22–C23	1.41(1)

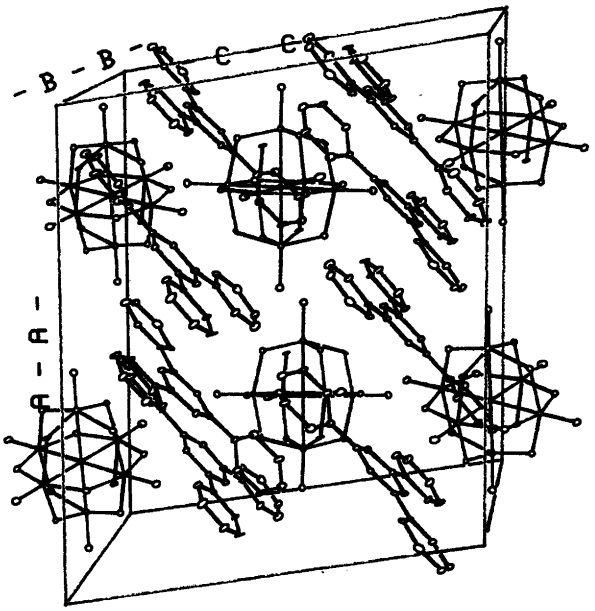

Fig. 5. View of crystal structure of $[TPP]_2Mo_6O_{19}$.

explained by C–C bond lengths and angles connecting the benzene rings with pyryllium. The two C–C bond lengths neighbouring the O atom are 1.43 and 1.44 Å, and are shorter than the equivalent bonds in **TPP–TCP**. The angles O(11)–C(1)–C(6) and O(11)–C(5)–C(18) [117.1(7) and 116(1)°], close to 120°, are larger than that of **TPP–TCP** (113.6 and 113.3°). The three benzene rings are planar within experimental error, and the rings of A and C are coplanar with the pyryllium ring. Ring B tilts from the plane of pyryllium at angles of 2.85, 25.25 and 3.14° for rings A, B and C, respectively. The results indicate that the pyryllium ring in **TPPM** tends to form a conjugated structure with two *ortho* benzene rings, and the electron deficit at C(1) and C(5) is higher than that at C(3).

In the unit cell, $Mo_6O_{19}^{2-}$ and **TPP** are arranged in the form of parallel columns along the ***c***-axis. The cations and anions stack alternately. The anions stack along the ***a***-axis, and the cations along the ***a***-direction inclining to the ***c***-axis. In the column, although the **TPP** cation is sandwiched by anions and *vice versa*, the **TPP** cation is alternately parallel in order, and its positive charge is in closer contact with one of the anions than the other. Thus the **TPP** cation and $Mo_6O_{19}^{2-}$ anion can be considered to form an ion-pair in the crystal as a column unit.

Acknowledgements. This work is supported by a grant for key research project from the State Science and Technology Commission and National Natura Science Foundation of China.

References

1. Ohashi, Y., Yanagi, K., Sasads, Y. and Yamase, T. *Bull. Chem. Soc. Jpn. 55* (1982) 1254 and references therein.
2. Prosser-Mccartha, C. M., Kadkhodayan, M., Williamson, M. M., Bouchard, D. A. and Hill, C. L. *J. Chem. Soc., Chem. Commun.* (1986) 1747.
3. Williamson, M. M., Bouchard, D. A. and Hill, C. L. *Inorg. Chem. 26* (1987) 1436.
4. Hill, C. L., Bouchard, D. A., Kadkhodayan, M., Williamson, M. M., Schmidt, J. A. and Hilinski, E. F. *J. Am. Chem. Soc. 110* (1988) 5471.
5. Attanasio, D., Bonamico, M., Fares, V., Imperatori, P. and Suber, L. *J. Chem. Soc., Dalton Trans.* (1990) 3221.
6. Attanasio, D., Bonamico, M., Fares, V. and Suber, L. *J. Chem. Soc., Dalton Trans.* (1992) 2523.
7. Xu, X.-X., You, X.-Z. and Wang, X. *Polyhedron 13* (1994) 1011.
8. Pope, M. T. and Muller, A. *Angew. Chem., Int. Ed. Engl. 30* (1991) 34.
9. Launay, J. P. *J. Inorg. Nucl. Chem. 38* (1976) 807.
10. Pope, M. T. *Heteropoly and Isopoly Oxometalates*, Springer, Berlin 1983.
11. Kraut, B. and Ferraudi, G. *J. Chem. Soc., Dalton Trans.* (1991) 2063.
12. Che, M., Fournier, M. and Launay, T. P. *J. Chem. Phys. 71* (1979) 1954.
13. Simalty, M. *Bull. Soc. Chim. Fr.* (1965) 1944.
14. Frenz, B. A. in Schenk, H., Olthof-Hazekamp, R., Vankoningsveld, H. and Bassi, G. C., eds., *Computing in Crystallography*, Delft University Press, Delft 19, pp. 64–71.
15. Fukutomi, H., Harazono, T. and Kojima, T. *Bull. Chem. Soc. Jpn. 59* (1986) 2387.
16. Wintgens, V., Pouliguen, J., Valt, P., Kossanyi, J., Canonica, S. and Wild, U. P. *Chem. Phys. Lett. 123* (1986) 735.
17. Miranda, M. A. and Garcia, H. *Chem. Rev. 94* (1994) 1063.
18. Fragst, F. and Ziebig, R. *Electrochim. Acta 23* (1978) 735.
19. Chen, Q. and Zubieta, J. *Coord. Chem. Rev. 114* (1992) 107.
20. Fuchs, S., Fretwald, W. and Hartl, H. *Acta Crystallogr., Sect. B 34* (1978) 1764.
21. Clegg, W. and Sheldrick, G. M. *Acta Crystallogr., Sect. B* (1982) 2906.
22. Tamamura, T., Yamane, T., Yasuoka, N. and Kasai, N. *Bull. Chem. Soc. Jpn. 47* (1974) 832.

Received December 30, 1994.